packing of the associated individuals suggest that this association is related to the biology of the organism rather than the result of inorganic processes in the depositional history of the rock. A general morphological similarity of these spheroids to resting zygotes of certain modern green algae (for example, *Chlamydomonas*) has been noted, inasmuch as the resting zygotes often form masses not unlike those observed in the fossil material.

The nonseptate filaments (Figs. 5 and 6) are unbranched, cylindrical amber filaments, 3 to 4 μ in diameter. The cell wall, approximately 0.5 μ thick, is of finely granular texture. The filaments frequently occur as sharply broken, short straight segments (Fig. 6), but they may occur as gently curved to sinuously wound threads (Fig. 5) more than 150 μ long. The filaments generally occur in clumps of subparallel orientation. Morphologically they may be compared to certain siphonalean green algae. However, no evidence of reproductive structures has been observed. As observed in transverse section, the filaments are almost perfectly circular in cross-sectional outline and show no signs of collapse or compression.

The small septate filaments (Figs. 1 and 4) are multicellular, unbranched, brownish-amber filaments tapering from a diameter of approximately 1.4 μ in the medial portion to a diameter of less than 1 μ toward the terminus; cells in the thicker portion of the filament are essentially isodiametric. Toward the terminus the cells are increasingly rectangular in longitudinal view; the terminal cell of the filament appears ellipsoidal (Fig. 1). Possibly these filaments, some of which are more than 75 μ long, were originally enclosed in an amorphous, hyaline sheath (Figs. 1 and 4). The tapering, possibly sheath-enclosed organization of these septate filaments of small diameter is strikingly similar to the morphology exhibited by certain modern blue-green algae (Oscillatoriaceae and Nostocaceae).

The large septate filaments (Figs. 2 and 3) are multicellular, unbranched, amber filaments, 2.3 to 3.4 μ in diameter. The cells vary in form from isodiametric to slightly elongate parallel to the long axes of the filaments. The filaments, some of which are more than 40 μ long, commonly have an irregularly granular surface texture (Fig. 3). An organic residue is often present within the cells (Fig. 2). In general appearance the larger filaments are very suggestive of certain modern green algae (for example, Ulotrichales).

Until further studies are made of the organic residues of these fossils—such as determination of their stable carbon isotope ratios and of their possible retention of the biologically significant hydrocarbons phytane and pristane—it is suggested, on morphological grounds alone, that we are dealing with a microflora of photosynthetic blue-green and green algae. The spatial relations of the microfossils to the laminations of the chert bands indicate that the organisms probably were growing at the time the silica was emplaced in shallow, possibly gently flowing, highly siliceous water. The exceptionally clear and relatively undistorted morphology of these minute organisms indicates that there has been little or no postdepositional metamorphism of the enclosing rock. As for their evolutionary and phylogenetic significance, certain of the microfossils are noteworthy as probable representatives of a transitional period in the evolution of Precambrian plant life during which the simpler green algae were diversifying.

ELSO S. BARGHOORN
J. WILLIAM SCHOPF
Biological Laboratories and *Botanical Museum, Harvard University, Cambridge, Massachusetts*

References and Notes

1. E. S. Barghoorn and S. A. Tyler, *Science* **147**, 563 (1965); S. A. Tyler and E. S. Barghoorn *ibid.* **119**, 606 (1954); J. W. Schopf, E. S. Barghoorn, M. D. Maser, R. O. Gordon, *ibid.* **149**, 1365 (1965); P. E. Cloud, Jr., *ibid.* **148**, 27 (1965); ——— and H. Hagen, *Proc. Natl. Acad. Sci. U.S.* **54**, 1 (1965); W. W. Moorhouse and F. W. Beales, *Trans. Roy. Soc. Can.* **56**, 97 (1962).
2. A. M. Macgregor, *Trans. Geol. Soc. S. Africa* **43**, 9 (1940).
3. S. A. Tyler, E. S. Barghoorn, L. P. Barrett, *Bull. Geol. Soc. Am.* **68**, 1293 (1957); J. Sederholm, *Compt. Rend. Congr. Intern. Geol. Stockholm* (1910); B. L. Stinchcomb, H. L. Levin, D. J. Echols, *Science* **148**, 75 (1965).
4. E. S. Barghoorn, W. G. Meinschein, J. W. Schopf, *Science* **148**, 461 (1965); W. G. Meinschein, E. S. Barghoorn, J. W. Schopf, *ibid.* **145**, 262 (1964); G. Eglinton, P. M. Scott, T. Belsky, A. L. Burlingame, M. Calvin, *ibid.*, p. 263.
5. H. Wopfner (Department of Mines, South Australia), personal communication, Apr. 1965.
6. We thank Dr. H. Wopfner of the South Australian Department of Mines, Adelaide, for allowing one of us (E.S.B.) to have access to recent unpublished maps of the Ross River area, and Dorothy Dellmer Barghoorn, Harvard University, for assistance in the field. This work was assisted by NSF grants GP 2794 and G-19727 to Harvard University. J.W.S. is an NSF graduate fellow.

13 August 1965

Hydrogen Emission Line $n_{110} \rightarrow n_{109}$: Detection at 5009 Megahertz in Galactic H II Regions

Abstract. *The hydrogen emission line* $n_{110} \rightarrow n_{109}$ *at the frequency 5009 megahertz which was predicted by Kardashev has been detected in M 17, Orion, and nine other galactic H II regions with the 42.7-m (140-foot) telescope and a 20-channel receiver at the National Radio Astronomy Observatory. The measured product of the half-power width of the line times the ratio of line-to-continuum brightness temperature is larger than that predicted by Kardashev's theory. The radial velocity obtained for M 17 and Orion agrees well with optical measurements. The search for a similar line of excited helium was without success.*

In 1959 Kardashev (*1*) pointed out that it should be possible to detect emission lines of hydrogen which were due to transitions between energy levels with very large quantum numbers n. He showed that in the recombination process occurring in H II regions the transitions $n \rightarrow (n-1)$ have the highest probability.

One of us tried in 1960 (*2*) to detect the line at 2.8 gigahertz, using the 25-m telescope of the University of Bonn, but could not pursue these observations because of lack of telescope time. In 1963 we started the development of a receiver at the National Radio Astronomy Observatory in order to search for the line. Part of a 20-channel receiver built for extragalactic 21-cm line observations (*3*) was incorporated in this receiver. A first series of observations with the NRAO 25.9-m (85-foot) telescope was started in the fall of 1964, but the results were too inconclusive to yield a positive detection of the line. In July 1965, the search for the line was resumed with a somewhat improved receiver, and with the recently completed NRAO 42.7-m (140-foot) telescope, having at 5 Ghz an effective antenna area about 2.7 times that of the 25.9-m telescope. The line was positively detected in M 17 during the first observation on July 9. Since then, observations of the line profiles of both thermal and nonthermal radio sources have been attempted. We give here a brief account of our observations of M 17, the Orion Nebula, Cygnus A, and Taurus A.

If we adopt the value $R = 3.2880559 \times 10^{15}$ hz for the Rydberg constant, the center frequency ν_L of the hydrogen line corresponding to the transition $n_{110} \rightarrow n_{109}$ becomes

$$\nu_L = R\left[\frac{1}{(n-1)^2} - \frac{1}{n^2}\right] = 5008.932 \text{ Mhz} \quad (1)$$

Kardashev (*1*) computed the product of line width $\Delta\nu_L$ times the line temperature T_L under the assumption of thermal equilibrium and that the line shape is gaussian (the half-power width of the line $\Delta\nu_L$ used in the following equations is related to the quantity $\Delta\nu_D$ used by Kardashev by $\Delta\nu_D = 0.6006\ \Delta\nu_L$):

$$\Delta\nu_L T_L = 1.67 \times 10^6 T_e^{-3/2} E \quad (2)$$

where T_e is the excitation temperature of the line, and E is the emission measure in parsec cm^{-6}. Taking the approximation for the absorption coefficient of free-free transitions given in (*4*) and assuming that the excitation temperature of the line is equal to the electron temperature, one obtains for the ratio of the brightness temperature T_L of the line to the brightness temperature T_C of an optically thin H II region with optical depth $\tau_C (T_C \approx \tau_C T_e)$

$$\left(\frac{\Delta\nu_L}{\text{hz}}\right)\frac{T_L}{T_C} = 2.01 \times 10^7 \left(\frac{\nu}{\text{Ghz}}\right)^{2.1} T_e^{-1.15}$$

It can be easily shown that, as long as the approximation $\exp[-(\tau_C + \tau_L)] \approx 1 - (\tau_C + \tau_L)$ holds, Eq. 3 is equal to the ratio $\Delta\nu_L(T_{C+L} - T_C)/T_C$ of the excess line-to-continuum brightness temperature times the bandwidth of the line. This quantity is observed directly. Note that Eq. 3 is somewhat different from the corresponding expression given in Kardashev's paper.

The block diagram of our line receiver is shown in Fig. 1. The system noise temperature including the antenna is about 450°K. A bandpass filter between the parametric amplifier (paramp) and mixer eliminates any ambiguity by suppressing the image frequency. The center frequency of the paramp can be tuned with the bias voltage. The input of the local oscillator (LO) multiplier is switched between two crystal-controlled oscillators. A noise tube is connected to the receiver input through a 20-db directional coupler; it can be operated in two different modes: (i) as a continuous calibration mark of 101.5°K and (ii) as a line calibration mark of 7.5°K. In the second case, the output noise is amplitude-modulated with the same frequency with which the LO is switched. After the intermediate frequency (IF) preamplifier the IF channels are split into (i) a broadband channel 8 Mhz wide, in which the total power of the source under investigation is measured, (ii) a line receiver which consists of 20 adjacent channels, each 100 khz wide with nearly square-shaped bandpass curves, and (iii) two channels with 400 and 800 khz bandwidth that are used for a preliminary search of the line.

Table 1. Quantitative results of the observations. All errors quoted are mean errors. Line temperatures are given in units of antenna temperature; rms, root mean square.

Source	T_L (°K)	T_L/T_C (%)	$\Delta\nu_L$ (khz) Obs.	$\Delta\nu_L$ (khz) Corr.	$\Delta\nu_L T_L/T_C$ (khz)	V(LSR) (km sec^{-1}) Radio	V(LSR) (km sec^{-1}) Optical
M 17	5.3 ± 0.45	7.15 ± 0.5	587 ± 30	577	42.0 ($\pm$ 9%)	$+ 17.7 \pm 2$	+ 21
Orion nebula	4.8 ± 0.40	6.57 ± 0.5	484 ± 30	474	31.8 ($\pm$ 9%)	$- 3.4 \pm 2$	+ 0.6
Cygnus	< 0.20 rms	< 0.22					
Taurus	< 0.29 rms	< 0.19					

In a typical set of observations the line profile observed on the source during 8 minutes is compared to the line profile of an off-source reference point, 5 minutes before and 5 minutes after the source observation. For the observations of strong sources, continuous noise is added to the antenna temperature of the off-source position in order to reduce the possible imbalance of the switched receiver due to different system noise temperatures on and off the source. (In the on-source position the source noise is added to the receiver noise.) The output data of the 20-channel receiver are recorded on magnetic tape and later processed in a computer. Figure 2 shows the results of our observations for four sources. The excited hydrogen line shows up quite clearly in the case of M 17 and the Orion nebula. The center frequency in Fig. 2, *a* and *b*, is the theoretical line frequency (Eq. 1), reduced to the local standard of rest (LSR), if the standard solar motion is 20.0 km/sec toward galactic longitude $l_{II} = 56.2°$ and galactic latitude $b_{II} = + 22.8°$. The velocity scale also refers to the LSR. Figure 2*c* shows the line profiles observed for Cygnus A and Taurus A. These sources, in which we did not expect to see the spectral line, were included in the observations as a check of the baseline of our spectrum analyzer. [We did not anticipate finding the excited hydrogen line in these two sources since (i) the sources are not predominantly thermal, (ii) their radial velocities lie outside the observed frequency region, and (iii) their turbulent velocities are probably so high that, even if H II were present, the resulting line would be too faint and too broad to be detected.] The scatter in the Cygnus A observation is obviously random, whereas in the Taurus A ob-

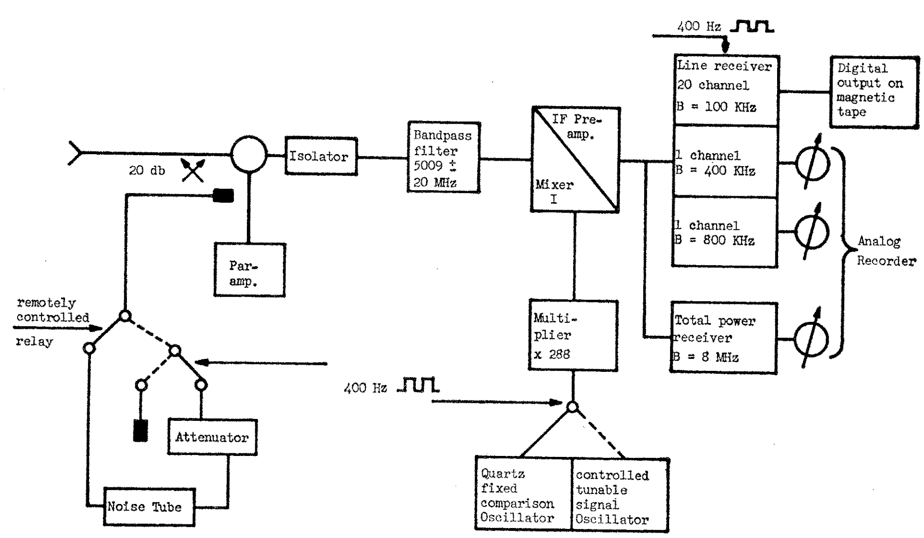

Fig. 1. Block diagram of the radiometer.

servations some systematic feature may be present. Gaussian curves have been fitted through the observed points in the results on Orion A and M 17 (Fig. 2, *a* and *b*). With both signal and comparison LO's fixed, the total analyzing bandwidth of the 20-channel receiver is 2 Mhz. During the various observations the signal LO was shifted occasionally in order to increase the effective frequency range of the observations. The integration times quoted in Fig. 2 refer to the total observing time on the source. Since the outer points in the profiles have been observed with a shorter integration time, their weights are smaller than those of the central points.

In the case of the Cygnus A and Taurus A observations, we insert for T_L the computed root-mean-square deviation from a straight line. The $\Delta\nu_L$ (corrected) is the observed line width corrected for the instrumental bandwidth. The accuracy of the temperature ratio T_L/T_C is greater than the accuracy of the absolute temperature value of T_L (which is given in units of antenna temperature) since T_L and T_C are measured relative to the same calibration mark.

Although Eq. 3 has been derived with the assumption that there is only Doppler broadening, the result should not be changed significantly if part of the line broadening is caused by collision broadening, and as long as no saturation effects occur. Evaluating Eq. 3 with the values given in Table 1, we obtain for the electron temperatures

$$T_e = 4.06 \begin{matrix} +0.43 \\ -0.38 \end{matrix} \times 10^3 \text{ deg K}$$

for M 17, and

$$T_e = 5.17 \begin{matrix} +0.43 \\ -0.38 \end{matrix} \times 10^3 \text{ deg K}$$

for Orion A. These values are lower than usually assumed. A more rigorous computation of both the absorption cross-section and the transition probabilities of the hydrogen atom is needed.

Kardashev also pointed out that for electrons at very high quantum levels line broadening due to Stark effect may be significant. However, as Kardashev himself pointed out, the approximate equations which he derives for the line broadening overestimate the influence of the Stark effect. If we evaluate his Eqs. 6, 7, and 8, putting $v_t = 0$ (that is, no turbulence), we obtain mean values of the electron density of the order of 50 cm^{-3}, which are at least one order of magnitude smaller than the electron densities derived for the central part of the Orion nebula and M 17 from measurements of the continuum radiation.

The radial velocities obtained from our radio measurements agree well with radial velocities derived from optical observations (*5*), considering the large uncertainty of the optical values. The period of observation is still too short for perception of a frequency shift caused by the earth's orbital motion.

Apart from the four sources discussed in this paper, the following sources have been investigated to date:

1) Positive detection of the excited hydrogen line: AMWW 30, A and B (W22); AMWW 37 (M 8); AMWW 42 (M 16); AMWW 51 (W43); AMWW 56A (W49); AMWW 58 A (W51); IC 434; IC 1795A. [AMWW refers to the 2.7-Ghz source catalog (*4*); W refers to the 1.4-Ghz source catalog given in (*6*). If observed with telescopes of high angular resolution, many of the strong galactic sources previously cataloged are resolved into clusters of individual sources. The nomenclature A, B, and so forth corresponds to the sequence of the relative intensities of the individual components of a cluster as observed with the 42.7-m telescope at 5 Ghz.]

2) Negative result: Cassiopeia A (although the scatter in its line profile is much larger than would be expected from statistical noise fluctuations alone); Centaurus A; Virgo A. These negative results were anticipated.

The results for the radio sources, observed by us up to now, in the Sagittarius region are not yet conclusive. It seems that these sources—if they are H II regions at all—have either extremely high radial velocities or very high internal motions, which result in a very strong line broadening.

Kardashev has also pointed out that similar emission lines should be found for the He atom. In the case of the hydrogen line observed here the frequency of the corresponding helium line should be 2.08 Mhz higher. Optical observations (*7*) yield a number ratio N_{He}/N_H of 0.13 for the Orion nebula. One would expect therefore a value of at least 0.62°K for the peak temperature of the helium line, provided that oscillator strength and transition probabilities of the He atom are similar to that of the H atom. We searched for this line in the Orion nebula without success. If there is a helium line present, its peak temperature is less than about 5 percent of that of the hydrogen line.

Two Russian groups have announced the detection of similar excited-hydrogen lines, but corresponding to different transitions. The Pulkovo group

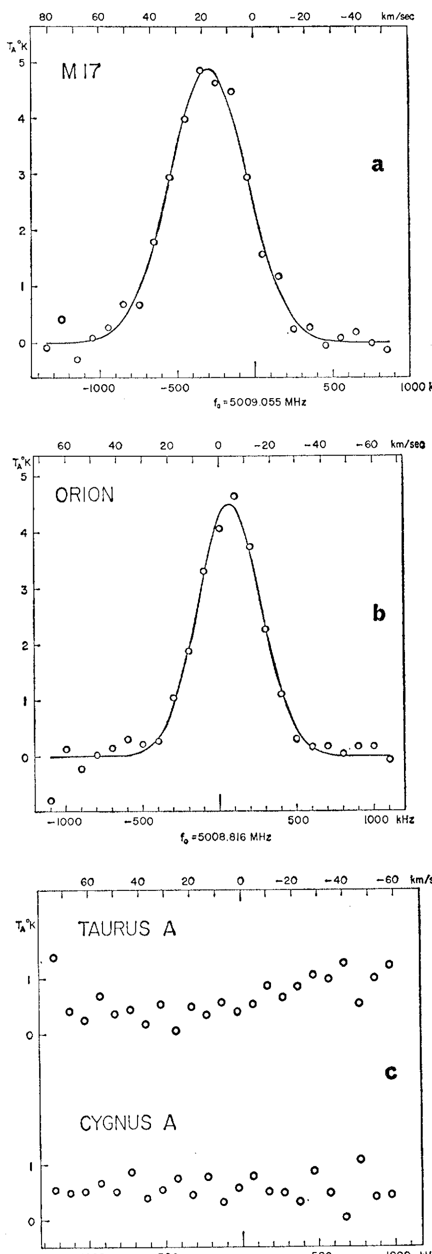

Fig. 2. *a*, Line profile of M 17; f_0 is the theoretical line frequency reduced to the local standard rest. The frequency and velocity scales are given with respect to LSR. Line temperature is given in units of antenna temperature. Integration time is 42 minutes. *b*, Line profile of the Orion nebula. Integration time is 133 minutes. *c*, Line profiles of Taurus A and Cygnus A. Integration times, 35 and 133 minutes, respectively. The frequency and velocity scales are given with respect to the theoretical line frequency (f_L).

has observed the line in M 17 and the Orion nebula at $\nu_L = 5736$ Mhz, corresponding to the transition $n_{105} \rightarrow n_{104}$ (*8*). Their quantitative values for M 17 ($T_L/T_C = 3.8 \pm 0.5$ percent, $\Delta\nu_L = 1.3 \pm 0.3$ Mhz) do not agree too well with our results. The Lebedev group observed the excited hydrogen line at $\nu_L = 8872.5$ Mhz, corresponding to the transition $n_{91} \rightarrow n_{90}$ (*9*). They found the line only in M 17 but, surprisingly, not in Orion A, and report for M 17 the result $T_L/T_C = 4.2 \pm 1.9$ percent, and $\Delta\nu_L = 1.3 \pm 0.3$ Mhz.

B. HÖGLUND
P. G. MEZGER
National Radio Astronomy Observatory, Green Bank, West Virginia

References and Notes

1. N. S. Kardashev, *Astron. J.* **36**, 838 (1959). Translated in *Soviet Astron.—AJ.* **3**, 813 (1960).
2. P. G. Mezger, *Veroeffentl. Univ. Sternwarte Bonn* Nr. **59**, 3 (1960).
3. B. Höglund and M. S. Roberts, in preparation.
4. W. Altenhoff, P. G. Mezger, H. Wendker, G. Westerhout, *Veroeffentl. Univ. Sternwarte Bonn* Nr. **59**, 48 (1960).
5. W. W. Campbell and J. H. Moore, *Univ. Calif. Publ. Lick Obs.* **13**, 282 (1918).
6. G. Westerhout, *Bull. Astron. Inst. Netherlands* **14**, 215 (1958).
7. J. S. Mathis, *Astrophys. J.* **125**, 328 (1957).
8. Z. V. D. Dravskikh and A. F. Dravskikh, *Astron. Zirk.* **282**, 2 (1964); Z. V. Dravskikh, A. F. Dravskikh, V. A. Kolbasov, *Intern. Astron. Union Gen. Assembly 12th, Hamburg, 1964.*
9. R. L. Sorochenko and E. V. Borodzich, *Intern. Astron. Union Gen. Assembly, 12th, Hamburg, 1964*, presented by V. V. Vitkevitch.
10. We thank the NRAO Electronic Division and especially N. Albaugh for construction and maintenance of the receiver; the telescope operators and mechanics at NRAO for help in making the observations; and colleagues on the staff for discussions. The National Radio Astronomy Observatory is operated by Associated Universities, Inc., under contract with NSF.

25 August 1965

Visual Contours in Homogeneous Space

Abstract. *With the aid of the Julesz figures, we introduce the concept of the stereoscopic edge, an edge which exists visually in the absence of physical contours. This edge, as well as the full complex of normal stereoscopy, can be present in the complete absence of physical contours at the fovea to approximately ± 3.00 degrees from fixation.*

In 1960, Julesz reported a new approach to the study of stereoscopic vision (*1*) which has led to the solution of many old problems by surprisingly simple means (*2, 3*). I would like to concentrate here on two issues which the Julesz figures have encouraged me to examine: one is the role of foveal contours in stereopsis and the second, more important, is the nature of the stereoscopic edge.

One term that must be defined is the *stereoscopic edge*. In classical stereograms, figural edges are almost invariably delineated by completed contours. If there are broken contours, they are not systematic nor analyzed as such. Figure and ground are fundamentally different. In the binary Julesz figures, on the contrary, figure and ground are equivalent and contours are invariably incomplete, in the Gestalt sense: if the figures are truly random, a contour line is as likely to be given by the triple of dots, black-white-black, as it is by any other permutation of three binaries. Nevertheless, the stereoscopic edge is as definite through the *white dots as it is through the black*.

This description of the Julesz figures is my own. I would like to point to its significance by asking "how big can the white (or, for that matter, the black) dots be?" Thus, "How much unstructured stereoscopic ground can there be between the figures?" Thus, "Is stereoscopic edge perception possible in or through a ground where there is nothing but undifferentiated white?" "Undifferentiated black?" "An empty visual Ganzfeld?"

The logic of the experiment is developed in Fig. 1*A*. This is a binary field in that the units are densely packed and are either black or white. More important, the units are of equal size and shape. The vertical columns consist of three bits. As a Julesz figure, let this pattern be that in the right eye, and let the pattern obtained by "moving the column marked δ over to the position marked δ′ and sliding the remaining columns the distance δ to the left" be that in the left eye. Since the bits are the same size, the horizontal retinal disparity (a function of δ) is basically constant over the field (*1*).

In Fig. 1*B*, however, I arbitrarily altered the horizontal dimensions of the bits. Nothing has changed from the point of view of information theory, since the topology has not changed (true also of Fig. 1*C* and Fig. 1*D*), but the retinal disparity is no longer constant over the field. Figure 1*C* shows a dilatation in the vertical direction. In this case, δ remains constant. Figure 1*D* combines both horizontal and vertical dilatations.

This experiment derives from Fig 1*C*, as illustrated in Fig. 1*E*. Since vertical

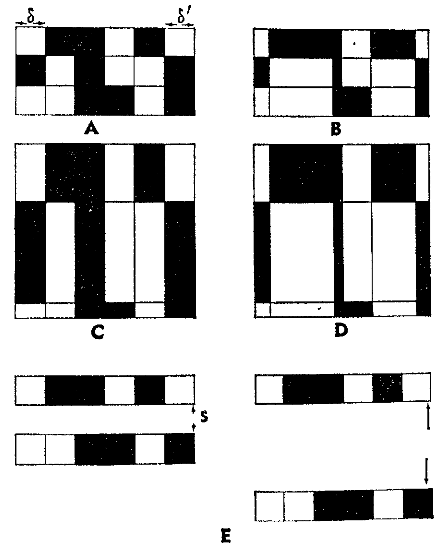

Fig. 1. The logic of the experiment.

dilatation leaves the retinal disparity constant, the middle row can be dropped and be replaced entirely with a homogeneous inner-region, either all light or all dark, of variable width *s*. Since neither the binary character of the Julesz figures nor their dense packing is essential, and since it is possible to keep δ acceptably small and reasonably constant by careful typesetting, it is feasible to use meaningful targets such as letters, numbers, diacritical signs, complex figurines, or what have you (see also *3*). Thus a target such as that in Fig. 2*A* was devised. It demonstrates a principle—as well as the possible relevance of this work to clinical ophthalmology—but *any* other target will do as well. The three uppermost and the three lowermost rows are nondisparate rows and thus provide a strong ground or reference plane; the four inner rows are disparate (δ = ♅ and δ′ = ⊕) but are otherwise identical so as to aid in the development of the figure or displaced plane. (Trials with nonidentical inner rows resulted in discrete, unevenly displaced planes. The careful observer may see that certain rows are still uneven!) A minimum number of rows is essential: an outer nondisparate pair, and an inner disparate pair (or vice versa, though the effect is less marked). I have used ten rows only as an experimental convenience. Without the nondisparate outer rows, the stereoscopic displacement occurs only indistinctly and certain ancillary perceptual effects (noted below) are absent.

The upper set of ten rows (two sets of five rows, side by side; one set for the left eye and one for the right) was photographically placed upon the upper